Use of the Discrete Fourier Transform in the Measurement of Frequencies and Levels of Tones

By D. C. RIFE and G. A. VINCENT

(Manuscript received May 7, 1969)

This paper considers the application of a digital computer and discrete Fourier transform (DFT) techniques to the measurement of signals known to comprise only single-frequency tones. We discuss the use of weighting functions to improve the effective selectivity of a measurement system that estimates the frequencies and levels of tones from the coefficients of their DFT. We present three classes of weighting functions which may be used to improve the inherent accuracy of such a system. The form of the weighting functions was chosen to minimize the amount of computer memory required, without using too much computer time. Several formulas are derived for estimating the frequency and level of a tone from its DFT coefficients. We chose the formulas to minimize computation time.

Simulation results indicate that, through the use of a proper weighting function, a DFT measurement system that uses 512 samples taken at a sampling frequency of 7040 Hz can be designed so that the maximum error in the frequency estimates of two tones near 1000 Hz and separated by approximately 50 Hz is about 0.03 Hz. The corresponding maximum error in the level estimate is on the order of 0.03 dB.

I. INTRODUCTION

There have been numerous articles, in recent years, dealing with the use of the discrete Fourier transform (DFT) in the area of spectrum analysis. Much of this interest was motivated by the availability of a computational algorithm that facilitates the rapid computation of DFT coefficients by a digital computer. The algorithm is, of course, the fast Fourier transform (FFT).

We are concerned with the problem of applying DFT techniques to the measurement of the levels and frequencies of single-frequency tones,

Fig. 1 — A DFT measurement system.

particularly tones from a data set during a test. Figure 1 shows the system we have in mind. A band-limited received signal, known to comprise one or more single-frequency tones, is periodically sampled by an A-D converter. A total of N samples are taken and the DFT coefficients are computed from the samples. The computer determines which of the DFT coefficients are "large", indicating the approximate frequencies of the received tones, and then proceeds to compute accurate estimates of the frequencies and levels. Methods for achieving the first part of the procedure are well known. This paper is devoted to a consideration of how best to go about the last step in the process, the accurate estimation of the frequencies and levels of the received tones.

In data set testing, the tone measurement system would be used occasionally during a test and would have to consume a minimum amount of real time. Thus we have directed our attention toward estimation methods that use simple formulas and require a minimum amount of computer memory.

Our attention is confined to the problem of leakage, its reduction by smoothing (windowing) functions, and the development of formulas which extract tone levels and frequencies from the list of DFT coefficients. We don't discuss the important, but secondary, problems of round-off errors and other noise sources.

II. REVIEW OF DISCRETE FOURIER TRANSFORM

The definition and properties of the discrete Fourier transform are discussed in Refs. 1 and 2. The following review is to refresh the reader's memory and establish the notation that we will use later.

2.1 *Definition of Discrete Fourier Transform*

Consider an ordered set of numbers $\{X_n\}$ where $n = 0, 1, 2, \cdots, N - 1$. Following Cochran, and others,[1] we define the discrete Fourier transform (DFT) of the set $\{X_n\}$ to be another set of numbers, $\{A_K\}$, with

$$A_K = \sum_{n=0}^{N-1} X_n e^{-j2\pi nK/N}, \quad \text{all integer} \quad K. \tag{1}$$

The inverse transformation is

$$X_n = \frac{1}{N} \sum_{K=0}^{N-1} A_K e^{j2\pi nK/N}, \qquad n = 0, 1, 2, \cdots, N-1. \tag{2}$$

2.2 *Useful Properties*

Several properties of the DFT are utilized in later parts of this paper. The important properties are recorded in this section for future reference. Reference 2 provides a more complete list. Derivations are included only for results that may not be well known.

From equation (1) it is obvious that if the X_n are real, then

$$A_{-K} = A_K^* \quad (* \text{ denotes conjugate}), \tag{3}$$

$$A_{K+N} = A_K, \tag{4}$$

and

$$A_{N-K} = A_{-K} = A_K^*. \tag{5}$$

2.2.1 *Convolution*

Let

$$B_K = \sum_{n=0}^{N-1} X_n e^{-j2\pi nK/N} \tag{6}$$

and

$$C_K = \sum_{n=0}^{N-1} Y_n e^{-j2\pi nK/N}, \tag{7}$$

then

$$A_m = \sum_{n=0}^{N-1} X_n Y_n e^{-j2\pi nm/N} = \frac{1}{N} \sum_{K=0}^{N-1} B_K C_{m-K}. \tag{8}$$

In other words, if $\{B_K\}$ and $\{C_K\}$ are the DFT of $\{X_n\}$ and $\{Y_n\}$, respectively, then the DFT of $\{X_n Y_n\}$ is given by equation (8).

2.2.2 *Power*

It can easily be shown, for X_n and A_K defined by equations (1) and (2), that

$$\frac{1}{N} \sum_{K=0}^{N-1} A_K A_K^* = \sum_{n=0}^{N-1} X_n^2. \tag{9}$$

If the X_n are samples of some function, $f(t)$; that is, if $X_n^2 = f^2(nT/N)$,

then

$$\lim_{N\to\infty} \frac{T}{N} \sum_{n=0}^{N-1} X_n^2 = \int_0^T f^2(t)\, dt$$

if the integral exists. Thus, for large N,

$$\int_0^T f^2(t)\, dt \approx \frac{T}{N} \sum_{n=0}^{N-1} X_n^2 . \tag{10}$$

Hence, from equation (9),

$$\frac{1}{T} \int_0^T f^2(t)\, dt \approx \frac{1}{N^2} \sum_{K=0}^{N-1} | A_K |^2. \tag{11}$$

2.3 *Relationship to Fourier Transform*

The DFT of samples of a signal has a simple relationship to the regular Fourier transform of the signal. It is instructive to examine this relationship.†

Let $g(t)$ be an arbitrary function, zero for $t < 0$ and $t > T$ and continuous over $0 < t < T$. The function is allowed to be discontinuous at $t = 0$ and at $t = T$. Assume that $g(0+)$ and $g(T-)$ exist.

A well-known application of the Poisson sum formula gives[4]

$$\tfrac{1}{2}g(0+) + \tfrac{1}{2}g(T-) + \sum_{n=1}^{N-1} g\left(\frac{nT}{N}\right) = \frac{N}{T} \sum_{n=-\infty}^{\infty} G\left(\frac{2\pi nN}{T}\right) \tag{12}$$

where

$$G(u) = \int_0^T g(t)e^{-iut}\, dt. \tag{13}$$

Adopting a notation similar to that of Papoulis,[4] we define the "#" operation by

$$G^{\#}(\omega) = \frac{N}{T} \sum_{K=-\infty}^{\infty} G(\omega - K\omega_s), \tag{14}$$

where

$$\omega_s = 2\pi N/T. \tag{15}$$

Then equation (12) can be rearranged to give

$$\sum_{n=0}^{N-1} g\left(\frac{nT}{N}\right) = G^{\#}(0) + \tfrac{1}{2}[g(0+) - g(T-)], \tag{16}$$

where $g(0)$ is taken to equal $g(0+)$.

† The recent article by Bergland touches upon this subject and also contains an extensive list of references.[3]

Let $h(t)$ be any function of the sort used above for $g(t)$ with the additional property: $h(0) = h(0+)$.

Let $s(t)$ be the signal to be analyzed and define

$$f(t) = s(t)h(t). \tag{17}$$

Let $g(t) = f(t)e^{-i\omega t}$ and define

$$A(\omega) = \sum_{n=0}^{N-1} f\left(\frac{nT}{N}\right)e^{-in\omega T/N}. \tag{18}$$

Then from equation (16) and the definition in equation (14) we have

$$A(\omega) = F^{\#}(\omega) + \tfrac{1}{2}[f(0+) - f(T-)e^{-i\omega T}], \tag{19}$$

where

$$F(\omega) = \int_0^T f(t)e^{-i\omega t}\, dt. \tag{20}$$

If $X_n = f(nT/N)$ then the A_K defined by equation (1) are given by

$$A_K = A\left(\frac{2\pi K}{T}\right). \tag{21}$$

Thus the DFT of the set $\{f(nT/N)\}$ are points along the curve described by equation (19). These points are $1/T$ Hz apart.

Observe that at $\omega = 2\pi K/T$ the term in brackets in equation (19) becomes $\frac{1}{2}[f(0+) - f(T-)]$ which is independent of K and vanishes if $f(0+) = f(T-)$.

2.4 *Weighting Functions*

If the DFT is to be taken of the set $\{s(nT/N)\}$ for $n = 0$ through $N - 1$, then $h(t)$ must be a function whose value is unity at $t = nT/N$; $n = 0, 1, \cdots, N - 1$. The function with this property that is usually taken to be $h(t)$ is the function $h_T(t)$;

$$h_T(t) = \begin{cases} 1, & 0 \leqq t < T; \\ 0, & \text{otherwise}. \end{cases} \tag{22}$$

Other weighting functions, $h(t)$, are often formed by multiplying $h_T(t)$ by a nontime-limited function. Weighting functions play a very important role in systems that use the DFT. The following paragraphs attempt to develop and present some of the pertinent theory.

From equation (19) we see the role that $F^{\#}(\omega)$ plays in $A(\omega)$. Since $f(t) = s(t)h(t)$,

$$F(\omega) = S(\omega) * H(\omega), \tag{23}$$

where the * denotes convolution and $S(\omega)$ and $H(\omega)$ are the Fourier transforms of $s(t)$ and $h(t)$. It can be shown that, subject to the usual convergence constraints,

$$F^{\#}(\omega) = [S(\omega)*H(\omega)]^{\#} = S(\omega)*H^{\#}(\omega). \tag{24}$$

Thus $H(\omega)$, or equivalently $H^{\#}(\omega)$, plays a central role in the DFT of (weighted) samples of $s(t)$. From the development that led to equations (19) and (21), we see that, if $h(0+) = h(T-)$, the DFT of samples of $h(t)$ is a set of points taken along the periodic curve described by $H^{\#}(\omega)$. It follows, therefore, that the values of $h(nT/N)$ can be obtained from

$$h\left(\frac{nT}{N}\right) = \frac{1}{N}\sum_{K=0}^{N-1} H^{\#}\left(\frac{2\pi K}{T}\right)e^{i2\pi Kn/N}. \tag{25}$$

Also,

$$H^{\#}(\omega) = \sum_{n=0}^{N-1} h\left(\frac{nT}{N}\right)e^{-jn\omega T/N} - \tfrac{1}{2}h(0+)[1 - e^{-j\omega T}]. \tag{26}$$

Weighting in the time domain is actually done at the points $t = nT/N$; $n = 0, 1, 2, \cdots, N-1$. For every set of weights to be applied at these points there exists a continuous function with the same values at the indicated time points. Thus there is no loss of generality due to discussing weighting in terms of weighting functions, $h(t)$, that are continuous over $(0, T)$ and zero outside that interval. We have to remember, however, that if the set $\{h(nT/N)\}$ is specified, $h(t)$ is not unique. Thus, if $H^{\#}(\omega)$ is given, $h(nT/N)$ is given by equation (25), but $h(t)$ and $H(\omega)$ are not uniquely defined.

There is apparently some confusion in the literature about whether $H(\omega)$ or $H^{\#}(\omega)$ is called a weighting function (or windowing function). Blackman and Tukey,[5] for example, discuss $h(t)$ and $H(\omega)$, but when Helms[6] writes about weighting with a Dolph-Chebychev function, he is evidently referring to $H^{\#}(\omega)$. More will be said about this later. Bingham, and others, in writing about data windows (See Reference 7, Part VII) mean $h(t)$.

Observe that $H^{\#}(\omega)$ is always periodic with period ω_s, while $H(\omega)$ is not periodic. (If it were, $H^{\#}(\omega)$ would not converge properly.) Generally the $H^{\#}(\omega)$ that one uses will have a prominent main lobe about $\omega = K\omega_s$ (K is any integer, including zero) and many side lobes. For our purposes it is important to obtain a narrow main lobe and low-amplitude side lobes.

The class of $H^{\#}(\omega)$ with the minimum main-lobe width for a given

side-lobe amplitude is known as the (discrete) Dolph-Chebyshev weighting functions.[8] A convenient form, similar to the one given by Helms,[6] but changed to describe the result of weighting by sample values that peak at $T/2$ and are adjusted to cover approximately unit area as later weighting functions will do, is the following:

$$H^*(\omega) = \frac{N}{R} e^{-j\omega T/2} \cos\left[N \cos^{-1}\left(Z_0 \cos\frac{\omega T}{2N}\right)\right] \tag{27}$$

where the side-lobe amplitude, $1/R$, is related to Z_0 by

$$R = \cosh\left(N \cosh^{-1} Z_0\right) \tag{28}$$

and N is the same as used in equation (1).

The class of $H(\omega)$ with the minimum main-lobe width for a given side-lobe amplitude is known as the continuous Dolph-Chebyshev functions,[9] which are unrealizable. The Taylor approximations to the continuous Dolph-Chebyshev functions[9-11] are realizable, however, and provide almost the same main lobe width for a given maximum side-lobe amplitude.

The problem of choosing "good" shapes for $H^*(\omega)$ can be approached by treating $H^*(\omega)$ or by treating $H(\omega)$. Most of the well-known weighting functions are discussed in terms of $H(\omega)$ or $h(t)$.

2.5 *A Generalization*

If $h(t)$ is a function that is zero for $t < T$, and $t > T$, then it can be shown (sampling theorem) that $H(\omega)$ is given by

$$H(\omega) = Te^{-j\omega T/2} \sin(\omega T/2) \sum_{n=-\infty}^{\infty} \frac{C_n}{\frac{\omega T}{2} - n\pi} \tag{29}$$

and

$$TC_n = H\left(\frac{2\pi n}{T}\right). \tag{30}$$

Thus the specification of a weighting function is equivalent to the specification of the constants, C_n.

III. SELECTED WEIGHTING FUNCTIONS

3.1 *Leakage and Aliasing*

Leakage will be used here to refer to the problem of the values of $A(\omega)$ due to $\cos(\omega_0 t + \theta_0)$ interferring with the values of $A(\omega)$ at some

other frequency, say ω_1, where the response due to $\cos(\omega_1 t + \theta_1)$ is to be examined. Leakage, in our system, is minimized by the use of weighting functions.

Aliasing refers to the fact that in a sampled-data system tones with frequencies above $\omega_s/2$ cannot be distinguished from tones with frequencies less than $\omega_s/2$. In our system aliasing is avoided by the use of the low-pass filter (Fig. 1).

3.2 *Convolution of Weighting Functions*

The object of weighting is to produce the DFT of a weighted set of samples of the signal undergoing measurement, $s(t)$. Thus we seek to compute

$$A_K = \sum_{n=0}^{N-1} s(nt_s)h(nt_s)e^{-j2\pi nK/N}, \quad \text{for all} \quad K; \tag{31}$$

where $t_s = T/N$. A convenient way of doing the weighting is to first compute

$$B_K = \sum_{n=0}^{N-1} s(nt_s)e^{-j2\pi nK/N}, \tag{32}$$

for $0 \leqq K \leqq N - 1$. Then if the set $\{H_m\}$,

$$H_m = \sum_{n=0}^{N-1} h(nt_s)e^{-j2\pi nm/N} = H^{\#}\left(\frac{2\pi m}{T}\right), \tag{33}$$

is stored in the computer, the A_K can be computed from equation (8).

3.3 *A Special Class of Weighting Functions*

The amount of computer memory required to store the set $\{H_m\}$ will be small if $h(t)$ is a function such that $H_m = 0$ for $M < |m| \leqq N/2$ and M is a relatively small number. The $H(\omega)$ corresponding to this class can be expressed by a particular form of equation (29):

$$H(\omega) = Te^{-iX} \sin X \sum_{n=-M}^{M} \frac{C_n}{X - n\pi}, \tag{34}$$

where

$$X = \omega T/2 \tag{35}$$

and $M \ll N/2$. We have restricted our attention to the results that can be obtained with this class of weighting functions.

Most of the well-known weighting functions, such as Hanning,[5] Hamming,[5] and Taylor[10,11] are in the class defined by equation (34).

The discrete Dolph–Chebychev and the Kaiser–Bessel[12] weighting functions, however, are not.

The right side of equation (34) can be written over a common denominator to obtain the form

$$H(\omega) = Te^{-iX}\frac{\sin X}{X}\frac{P(X)}{\prod_{n=1}^{M}(X^2 - n^2\pi^2)}, \tag{36}$$

where $P(X)$ is, in general, a complex polynomial in X. We will restrict our attention to $H(\omega)$ with real C_n and $C_0 = 1$. In which case $C_{-n} = C_n$ and, if $D_n = 2C_n$, we have

$$h(t) = h_T(t)\left[1 + \sum_{n=1}^{M} D_n \cos\left(\frac{2\pi nt}{T}\right)\right]. \tag{37}$$

Equation (34) becomes

$$H(\omega) = Te^{-iX}\sin X\left[\frac{1}{X} + \sum_{n=1}^{M}\frac{D_nX}{X^2 - n^2\pi^2}\right]. \tag{38}$$

In the next few sections we will discuss three classes of weighting functions with the form of equations (37) and (38). They were chosen to provide two extreme cases of weighting and an intermediate example. Many other weighting functions in the class defined by equations (37) and (38) exist; the ones examined below provide sufficient data for our purposes.

3.4 *Class I Weighting Functions*

We first consider the class of weighting functions that provides the best possible reduction in $|H(\omega)|$ for large ω. Let this class be known as Class I.

The only part of equation (36) that can be adjusted is the polynomial, $P(X)$. Thus we must choose the coefficients, D_n, to minimize $|P(X)|$ for large X. This is done by forcing $P(X)$ to be a constant. The constant term in $P(X)$, from equation (34), is

$$P(0) = (-1)^M\pi^{2M}(M!)^2. \tag{39}$$

Hence, the desired class of weighting functions has the form, from equation (36),

$$H_M(\omega) = Te^{-iX}\frac{\sin X}{X}\frac{(-1)^M\pi^{2M}(M!)^2}{\prod_{n=1}^{M} X^2 - n^2\pi^2}. \tag{40}$$

We denote the coefficients, D_n, of this class of weighting functions as $D_I(M, n)$, making the dependence upon M explicit. From equations (36), (38), and (40) the $D_I(M, n)$ are given by

$$D_I(M, n) = \lim_{X \to n\pi} \frac{(-1)^M \pi^{2M} (M!)^2 (X^2 - n^2\pi^2)}{X^2 \prod_{K=1}^{M} X^2 - K^2\pi^2}. \tag{41}$$

Evaluation of the limit and some simplification gives

$$D_I(M, n) = \frac{2(-1)^n (M!)^2}{(M - n)!\,(M + n)!} = 2(-1)^n \prod_{K=1}^{n} \frac{M + 1 - K}{M + K}. \tag{42}$$

We denote the weighting functions that use equation (41) as $h_M(t)$. Then from equation (37)

$$h_M(t) = h_T(t)\left[1 + \sum_{n=1}^{M} D_I(M, n) \cos \frac{2\pi n t}{T}\right]. \tag{43}$$

This can easily be shown to be the same as

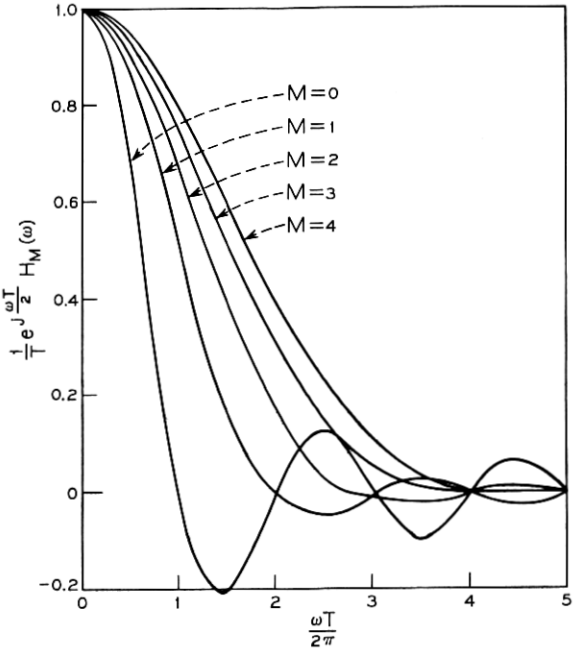

Fig. 2 — Spectra of the Class I weighting functions.

$$h_M(t) = h_T(t) \frac{4^M (M!)^2}{(2M)!} \sin^{2M}\left(\frac{\pi t}{T}\right). \tag{44}$$

Thus the Class I weighting functions are described by equations (40) and (44). The so-called *hanning* weighting[5] is equivalent to $h_1(t)$. Larsen and Singleton[13] used $h_1(t)$, $h_2(t)$, and others.

Fig. 2 shows the shape of $(1/T)e^{i\omega T/2}H_M(\omega)$ for M up to 4. In Fig. 3 we have plotted the normalized transmission of $H_M(\omega)$ (that is, 20 Log_{10} $(H_M(\omega)/T|)$. Several of the $h_M(t)$ are shown in Fig. 4 and some values of $D_I(M, n)$ have been tabulated in Table I.

3.5 *Class II Weighting Functions (Taylor)*

Class I weighting functions provide the minimum high-order side-lobe amplitude in $H(\omega)$ that is possible with a given value of M. We now turn to the class that gives the minimum main-lobe width, at the expense of higher side-lobe amplitude.

The so-called continuous Dolph–Tchebycheff weighting functions[8]

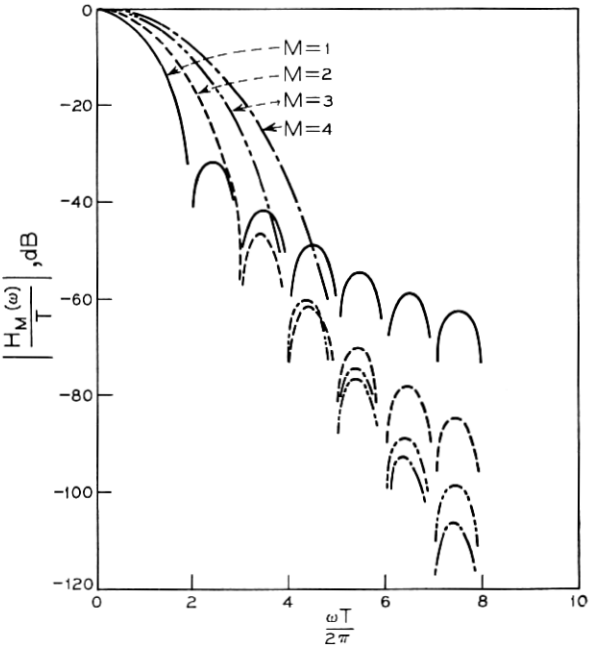

Fig. 3 — Normalized loss of the Class I weighting functions.

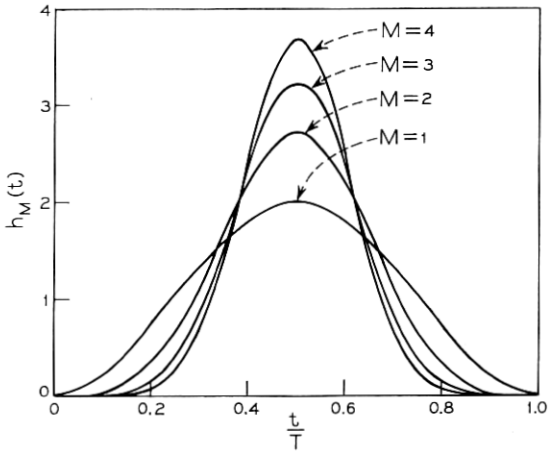

Fig. 4 — Time response of the Class I weighting functions.

provide the minimum main-lobe width in $H(\omega)$, consistent with a specified maximum side-lobe amplitude, but they are unrealizable functions. The Taylor[10] approximation to the Dolph–Tchebycheff functions provides almost the same main-lobe width and side lobes that have the specified maximum amplitude near the main lobe and then gradually decrease as ω increases.

The Taylor functions have the form given by equations (37) and (38) with the D_n dependent upon M and the maximum side-lobe amplitude, $1/R$. We will denote the D_n coefficients of Taylor weighting by $D_{II}(R, M, n)$, making the dependence upon R explicit. After adapting Taylor's equations to our situation, the D_{II}'s are given by

$$D_{II}(R, M, n) = -\frac{\prod_{K=1}^{M}\left[1 - \frac{(n/\sigma)^2}{\lambda^2 + (K - \frac{1}{2})^2}\right]}{\prod_{\substack{K=1 \\ K\neq n}}^{M}\left[1 - \left(\frac{n}{K}\right)^2\right]}, \tag{45}$$

where

$$R = \cosh(\pi\lambda) \tag{46}$$

and

$$\sigma^2 = \frac{(M + 1)^2}{\lambda^2 + (M + \frac{1}{2})^2}. \tag{47}$$

TABLE I —VALUES OF $D_I(M, n)$ FOR M UP TO 4

M	n			
	1	2	3	4
1	−1	—	—	—
2	−4/3	1/3	—	—
3	−3/2	3/5	−1/10	—
4	−8/5	4/5	−8/35	1/35

Solving equation (46) for λ gives

$$\lambda = \frac{1}{\pi} \ln [R + \sqrt{R^2 - 1}]. \tag{48}$$

We will refer to the Taylor functions described by equations (45) through (48) as Class II weighting functions and denote them by $k_M(R, t)$ and $K_M(\omega)$. References 10 and 11 give a further discussion of Taylor functions. Taylor weighting functions have the property that, if M is too small, the D's given by equations (45) will define an $H(\omega)$ whose first few side lobes have the amplitude given by equation (46), but some of the higher-order side lobes will have much higher amplitudes. Thus, for each value of desired side-lobe level, $1/R$, there is a minimum value of M that will give good side-lobe suppression.

Some minimum values of M that give good side-lobe control are listed in Table II.

Figures 5 and 6 show the shapes of a Class II weighting function with $M = 7$ and $R = 10^3$. This particular weighting function will be examined below when simulation results are compared. It will be shown there that this weighting function is useful when the received tone frequencies are very closely spaced.

3.6 *Class III Weighting Functions*

The third class of weighting functions has been chosen to have, to a

TABLE II—MINIMUM VALUES OF M FOR GOOD SIDE-LOBE CONTROL

$20 \log_{10} R$ (db)	M
36	3
42	4
48	5
54	6
60	7
66	9

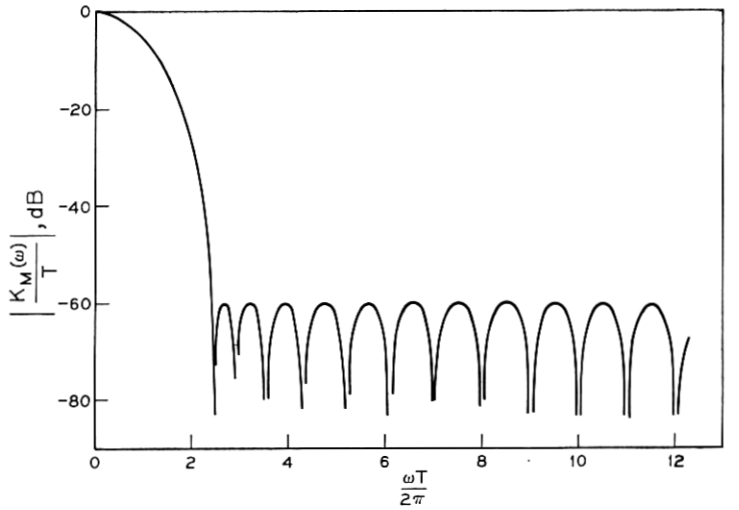

Fig. 5 — Normalized loss of the Class II weighting functions.

large extent, the desirable properties of both Class I and Class II weighting functions. That is, Class III weighting provides better resolution than Class I weighting for tones with a "small" frequency separation. Moreover, they also provide better resolution than Class II weighting of tones with a "large" frequency separation.

We will identify the Class III weighting functions by $g_M(t)$ and $G_M(\omega)$, where $g_M(t) \leftrightarrow G_M(\omega)$. The D_n coefficients for this class will be denoted by $D_{III}(M, n)$. The first member of the class is chosen as dis-

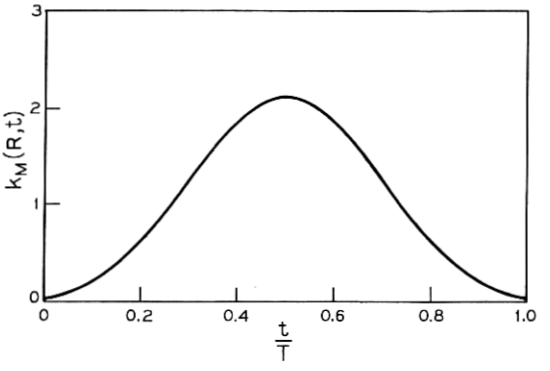

Fig. 6 — Time response of the Class II weighting functions; $M = 7$, $R = 1000$.

cussed below and the other members are obtained by operations on the first.

In order to have the high-order side lobes of $G_M(\omega)$ fall off at least as $1/\omega^2$ we must have $g_M(0+) = g_M(T-) = 0$. In terms of the D_n values this means that

$$1 + \sum_{n=1}^{M} D_{III}(M, n) = 0. \tag{49}$$

With this restriction, of course, $g_1(t)$ is the same as the Class I weighting function, $h_1(t)$. Thus the distinguishing properties of Class III weighting are determined by $g_2(t)$.

We chose the coefficients of $g_2(t)$ so that the loss of $G_2(\omega)$ reached 60 dB with as small a value of ω as possible with the side lobes of $G_2(\omega)$ never exceeding -60 dB, subject to equation (49). The D_n values for this condition are:

$$D_{III}(2, 1) = -1.19685, \qquad D_{III}(2, 2) = 0.19685.$$

The $g_2(t)$ thus defined is almost the same as Blackman's[5] proposed function, $Q_4(f)$.

The rest of the members of the Class III functions are defined in a manner similar to that used by Helms[6] for the synthesis of digital filters. We define

$$g_M(t) = \frac{h_{M-2}(t) g_2(t)}{1 + \frac{1}{2} D_{III}(2, 1) D_I(M - 2, 1) + \frac{1}{2} D_{III}(2, 2) D_I(M - 2, 2)}, \qquad M > 2. \tag{50}$$

The normalization in equation (50) puts $g_M(t)$ in the form of equation (37).

The Class III functions just defined have high-order side lobes, in $G_M(\omega)$, that decrease as ω^{-M}. This contrasts with $\omega^{-(M+1)}$ for Class I weighting and with ω^{-1} for Class II weighting. Thus, Class III weighting functions provide slightly narrower main-lobe width than Class I at the expense of slightly higher side lobes.

Some values of $D_{III}(M, n)$ are tabulated in Table III.

In Fig. 7 we have plotted the normalized spectra (that is, $(1/T)e^{j\omega T/2}G_M(\omega)$) of some Class III weighting functions. Fig. 8 illustrates the normalized loss provided by $G_M(\omega)$ for values of M up to 4. It is interesting to note, from Fig. 7, that $G_2(\omega)$ reaches -50 dB before any of the others, just as $H_2(\omega)$ did in Fig. 3. In Fig. 9 we have plotted $g_M(t)$ for values of M up to 4.

TABLE III—VALUES OF $D_{III}(M, n)$ FOR M UP TO 4

	n			
M	1	2	3	4
2	−1.19685	.19685	—	—
3	−1.43596	.497537	−.0615762	—
4	−1.566272	.725448	−.180645	.0179211

IV. RESPONSE TO A COSINE WAVE

We are interested in measuring the frequencies and levels of signals that comprise several sine waves. In view of this and the linearity of the DFT it is convenient to examine the properties of the DFT of samples of cos $(\omega_0 t + \theta)$.

4.1 *Basic Formulas*

Let

$$s(t) = \cos(\omega_0 t + \theta) \tag{51}$$

$$f(t) = h_T(t) \cos(\omega_0 t + \theta). \tag{52}$$

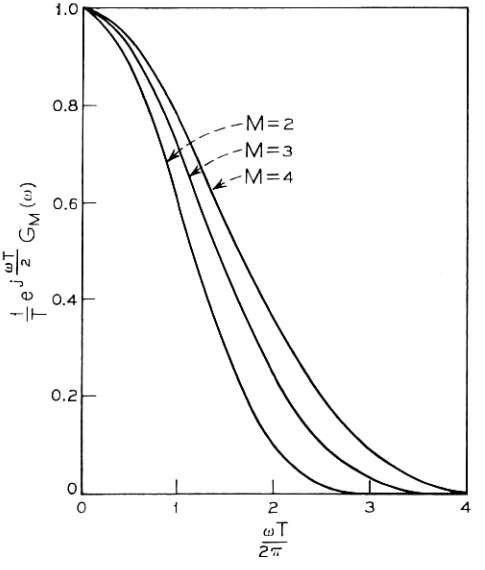

Fig. 7 — Spectra of the Class III weighting functions.

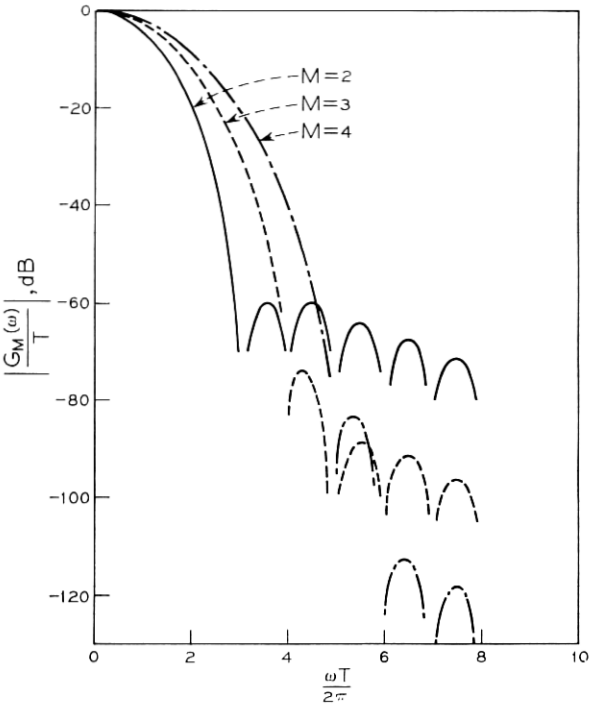

Fig. 8 — Normalized loss of the Class III weighting functions.

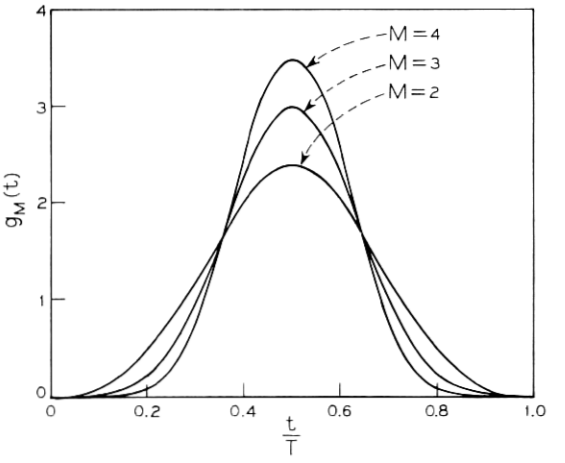

Fig. 9 — Time response of the Class III weighting functions.

and

$$H_T(\omega) = \int_{-\infty}^{\infty} h_T(t)e^{-i\omega t}\, dt \tag{53}$$

or, in the usual notation,

$$H_T(\omega) \leftrightarrow h_T(t). \tag{54}$$

Then

$$F^*(\omega) = \tfrac{1}{2}e^{i\theta}H_T^*(\omega - \omega_0) + \tfrac{1}{2}e^{-i\theta}H_T^*(\omega + \omega_0) \tag{55}$$

and from equation (19)

$$A(\omega) = \tfrac{1}{2}e^{i\theta}H_T^*(\omega - \omega_0) + \tfrac{1}{2}e^{-i\theta}H_T^*(\omega + \omega_0) + \tfrac{1}{2}[\cos\theta - \cos(\omega_0 T + \theta)e^{-i\omega T}]. \tag{56}$$

With $h_T(t)$ as defined by equation (22)

$$H_T(\omega) = Te^{-i\omega T/2}\frac{\sin(\omega T/2)}{\omega T/2}. \tag{57}$$

It is possible to put equation (57) in equation (56) and evaluate the indicated summations. The same answer can, however, be found more easily from equation (18). With equation (52) in equation (18) we have

$$A(\omega) = \sum_{n=0}^{N-1} \cos\left(\frac{\omega_0 nT}{N} + \theta\right)e^{-jn\omega T/N} \tag{58}$$

or

$$A(\omega) = \tfrac{1}{2}e^{j\theta}\sum_{n=0}^{N-1} e^{-j(\omega-\omega_0)nT/N} + \tfrac{1}{2}e^{-j\theta}\sum_{n=0}^{N-1} e^{-j(\omega+\omega_0)nT/N}. \tag{59}$$

Both sums in equation (59) are finite geometric series. Thus after rearrangement we obtain

$$A(\omega) = \tfrac{1}{2}e^{j\theta}e^{-j(N-1)z}\frac{\sin Nz}{\sin z} + \tfrac{1}{2}e^{-j\theta}e^{-j(N-1)y}\frac{\sin Ny}{\sin y} \tag{60}$$

where

$$z = \frac{(\omega - \omega_0)T}{2N} \tag{61}$$

and

$$y = \frac{(\omega + \omega_0)T}{2N}. \tag{62}$$

The formulation given by equation (56) is important from a conceptual point of view while that of equation (60) is useful for numerical evaluations.

The evaulation of equation (60) when either z or y is zero requires an examination of limits, which can be done by inspection.

4.2 *General* $A(\omega)$

The use of one of the weighting functions defined by equations (34), (37), and (38) gives rise to an $A(\omega)$ different from the one calculated in equation (60). The more generalized form of $A(\omega)$ is given by

$$A(\omega) = \tfrac{1}{2}e^{j\theta}e^{-jNz}\sin Nz \sum_{n=-M}^{M} C_n \frac{e^{j(z-n\pi/N)}}{\sin\left(z - \frac{n\pi}{N}\right)} + \tfrac{1}{2}e^{-j\theta}e^{-jNy}\sin Ny \sum_{n=-M}^{M} C_n \frac{e^{j(y-n\pi/N)}}{\sin\left(y - \frac{n\pi}{N}\right)}. \tag{63}$$

All of the simulations, to be discussed below, used this $A(\omega)$, in equation (21), to compute A_K values.

4.3 *Approximations*

We will make use of several approximations in the next section. The important ones are established here. In this section $h_T(t)$ is assumed to be the weighting function and ω is in the range $0 < \omega < \omega_s/2$.

Consider equation (19). If $| F(\omega - l\omega_s) |$ is small for $l \neq 0$; then

$$A(\omega) \cong \frac{1}{t_s} F(\omega) + \tfrac{1}{2}[f(0+) - f(T-)e^{-j\omega T}] \tag{64}$$

where

$$t_s = T/N. \tag{65}$$

Thus, from equation (21),

$$A_K \cong \frac{1}{t_s} F\left(\frac{K\omega_s}{N}\right) + \tfrac{1}{2}[f(0+) - f(T-)]. \tag{66}$$

Next consider equations (56) and (57). $| H_T(\omega) |$ is "large" only near $\omega = 0$. Thus we obtain another approximation, used when $s(t) = \cos(\omega_0 t + \theta)$,

$$F(\omega) \approx \tfrac{1}{2}e^{j\theta}H_T(\omega - \omega_0). \tag{67}$$

From equation (57) we then obtain

$$\frac{1}{t_s} F(\omega) \cong \frac{N}{2} e^{j\theta} e^{-j[(\omega-\omega_0)T/2]} \frac{\sin [(\omega - \omega_0)T/2]}{[(\omega - \omega_0)T/2]}. \tag{68}$$

Thus,

$$| A_K | \cong \frac{N}{2} \frac{\left| \sin \left(\frac{K\omega_s T}{2N} - \frac{\omega_0 T}{2} \right) \right|}{\left| \left(\frac{K\omega_s T}{2N} - \frac{\omega_0 T}{2} \right) \right|} \tag{69}$$

or, because,

$$\frac{K\omega_s T}{2N} = K\pi, \tag{70}$$

$$| A_K | \cong \frac{N}{2} \frac{\left| \sin \left(K\pi - \frac{\omega_0 T}{2} \right) \right|}{\left| \left(K\pi - \frac{\omega_0 T}{2} \right) \right|}. \tag{71}$$

From equation (71) we see that, apart from the error in the approximations, one should be able to accurately estimate the frequency and magnitude of a cosine wave from the A_K values for K near $\omega_0 T/2\pi$.

The main lobe of a $\sin X/X$ curve reaches zero at $X = \pm\pi$. Thus the main lobe of the curve, of which the A_K are points, reaches zero at $\omega = \omega_0 \pm 2\pi/T$ or, since $\omega_s/N = 2\pi/T$, at

$$\omega = \omega_0 \pm \omega_s/N.$$

The main lobe is just wide enough to contain two A_K values (estimators), except if ω_0 equals some multiple of ω_s/N. It will be shown later that two A_K values will be enough to estimate the parameters of a cosine wave.

V. FREQUENCY AND LEVEL ESTIMATION

In the preceding sections we have developed methods of computing the DFT coefficients of a known input (for simulations) and have discussed three classes of weighting functions to improve the effective selectivity of the DFT process. Our final task, which is undertaken in this section, is to determine accurate ways of processing the DFT coefficients to extract the frequencies and magnitudes present in the sampled signal.

The methods are to be useful when the real-time demands upon the

computer are important. Thus all of the methods were chosen to have simple formulas which the computer can be programmed to evaluate when it is making a measurement.

The equations we have examined fall into two classes: those that use only two estimators to calculate the frequency and level of a cosine wave and those that use many. The following paragraphs derive the most promising of these equations. The next section will present the accuracies that the various equations can achieve. We start with a formula that makes use of many estimators.

5.1 *Method 1*

The derivation of this method is somewhat involved, so we first explain the motivation behind it.

Suppose one has an $f(t)$ that is known to be given by

$$f(t) = B \cos \omega_0 t, \tag{72}$$

and one wants to determine ω_0 and B from operations on $f(t)$. One way to determine B is from

$$\begin{aligned} \lim_{T\to\infty} \frac{1}{T} \int_0^T f^2(t)\, dt &= \lim_{T\to\infty} \frac{1}{T} \int_0^T B^2/2\, dt \\ &= B^2/2 \end{aligned} \tag{73}$$

thus,

$$B^2 = 2 \lim_{T\to\infty} \frac{1}{T} \int_0^T f^2(t)\, dt. \tag{74}$$

The derivative of $f(t)$ is

$$f'(t) = -B\omega_0 \sin \omega_0 t \tag{75}$$

and

$$\lim_{T\to\infty} \frac{1}{T} \int_0^T [f'(t)]^2\, dt = B^2\omega_0^2/2 \tag{76}$$

Thus ω_0 can be determined from

$$\omega_0^2 = \frac{\lim_{T\to\infty} \frac{1}{T} \int_0^T [f'(t)]^2\, dt}{\lim_{T\to\infty} \frac{1}{T} \int_0^T [f(t)]^2\, dt}. \tag{77}$$

The above result is the motivation for the following derivation.

Assume

$$s(t) = B \cos (\omega_0 t + \theta) \tag{78}$$

and

$$f(t) = h(t)B \cos (\omega_0 t + \theta) \tag{79}$$

where $h(t)$ is one of the weighting functions, given by

$$h(t) = \left[1 + \sum_{n=1}^{M} D_n \cos \left(\frac{2\pi n t}{T}\right)\right] h_T(t). \tag{80}$$

Let the estimators, A_K, be given by equation (31).

Define

$$P_0 = \lim_{T\to\infty} \frac{1}{T} \int_0^T [f(t)]^2 \, dt \tag{81}$$

and

$$P_1 = \lim_{T\to\infty} \frac{1}{T} \int_0^T [f'(t)]^2 \, dt. \tag{82}$$

Expansion of equation (79) gives

$$f(t) = Bh_T(t)\Big\{\cos (\omega_0 t + \theta) + \frac{1}{2} \sum_{n=1}^{M} D_n[\cos (\omega_0 t - n\omega_a t + \theta) + \cos (\omega_0 t + n\omega_a t + \theta)]\Big\} \tag{83}$$

where

$$\omega_a = 2\pi/T. \tag{84}$$

From equations (81) and (83)

$$P_0 = \frac{B^2}{2}\left\{1 + \frac{1}{2} \sum_{n=1}^{M} D_n^2\right\}. \tag{85}$$

Calculation of P_1 from equation (83) yields, assuming $n\omega_a \neq \omega_0$,

$$P_1 = \frac{B^2}{2}\left\{\omega_0^2 + \sum_{n=1}^{M} \frac{D_n^2\omega_0^2}{2} + \sum_{n=1}^{M} \frac{n^2 D_n^2 \omega_a^2}{2}\right\}. \tag{86}$$

Combining equations (85) and (86) gives

$$\omega_0^2 = \frac{P_1}{P_0} - \frac{\omega_a^2 \sum_{n=1}^{M} n^2 D_n^2}{2 + \sum_{n=1}^{M} D_n^2}. \tag{87}$$

The next step is to compute P_1/P_0 from the DFT of $f(t)$. Using the approximation

$$f(t) \approx \frac{h_T(t)}{N} \sum_{k=-N/2}^{N/2} A_K e^{jK\omega_a t} \tag{88}$$

which can be rearranged to give

$$f(t) \approx \frac{h_T(t)}{N} \left\{ A_0 + 2 \sum_{K=1}^{N/2} [\mathrm{Re}\,(A_K) \cos K\omega_a t - \mathrm{Im}\,(A_K) \sin K\omega_a t] \right\}. \tag{89}$$

From equation (89)

$$P_0 \approx \frac{1}{N^2} \left\{ A_0^2 + 2 \sum_{K=1}^{N/2} | A_K |^2 \right\} \tag{90}$$

and

$$P_1 \approx \frac{1}{N^2} \sum_{K=1}^{N/2} 2 | A_K |^2 K^2 \omega_a^2 . \tag{91}$$

Thus,

$$\frac{P_1}{P_0} \approx \frac{\omega_a^2 \sum_{K=1}^{N/2} K^2 | A_K |^2}{\frac{A_0^2}{2} + \sum_{K=1}^{N/2} | A_K |^2} . \tag{92}$$

We use equation (92) in equation (87) to obtain the final result. Denote the estimated ω_0 by $\hat{\omega}_0$. Then

$$\hat{\omega}_0^2 = \omega_a^2 \left\{ \frac{\sum_{K=1}^{N/2} K^2 | A_K |^2}{\frac{1}{2} A_0^2 + \sum_{K=1}^{N/2} | A_K |^2} - U_M \right\} \tag{93}$$

where

$$U_M = \frac{\sum_{n=1}^{M} n^2 D_n^2}{2 + \sum_{n=1}^{M} D_n^2} \tag{94}$$

By D_n we mean, of course, $D_{\mathrm{I}}(M, n)$, $D_{\mathrm{II}}(R, M, n)$ or $D_{\mathrm{III}}(M, n)$. Thus Method 1 is applicable to all three classes of weighting functions. Some values for U_M are tabulated in Table IV.

TABLE IV—VALUES OF U_M AND V_M

Class I Weighting

M	U_M	V_M
0	0	.5
1	.333333	.75
2	.571429	.972222
3	.818182	1.155
4	1.06667	1.31327

Class II Weighting

($M = 7$, $R = 1000$)

$U_7 = .357071$, $V_7 = .769710$

Class III Weighting

M	U_M	V_M
2	.45732	.8678
3	.715523	1.07833
4	.968949	1.25033

The way to use equation (93), when more than one tone is present in $s(t)$, is to use only the estimators, A_K, for $K \approx \omega_0/\omega_a$ to calculate each $\hat{\omega}_0$. The simulations below will show that this technique gives accurate results.

5.1.1 *Estimation of Level*

From equations (85) and (90), we obtain the way to estimate B.

$$\hat{B}^2 = \frac{1}{N^2} \frac{A_0^2 + 2 \sum_{K=1}^{N/2} | A_K |^2}{V_M} \tag{95}$$

where

$$V_M = \tfrac{1}{2} + \tfrac{1}{4} \sum_{n=1}^{M} D_n^2 . \tag{96}$$

Some values of V_M are tabulated in Table IV. Observe that if only the basic weighting, $h_T(t)$, is used, then U_M and V_M become zero and $\frac{1}{2}$, respectively.

5.2 *Method 2*

The preceding formulas for estimating the frequency and level of a cosine wave from its DFT use more than two estimators. The next few paragraphs establish formulas that require only two estimators. The formulas apply only to the Class I weighting functions, $h_M(t)$.

We start by recalling the approximations given by equations (64) and (67). With $H_M(\omega)$ substituted for $H_T(\omega)$ in equation (67) we have

$$A(\omega) \approx \frac{1}{2t_s} e^{j\theta} H_M(\omega - \omega_0). \tag{97}$$

From equation (40)

$$H_M\left(\frac{2X}{T}\right) = T e^{-iX} \frac{\sin X}{X} \frac{(-1)^M \pi^{2M} (M!)^2}{\prod_{n=1}^{M} (X^2 - n^2\pi^2)} \tag{98}$$

where $X = \omega T/2$. If $s(t) = B \cos(\omega_0 t + \theta)$ then, from equations (97) and (98),

$$| A(\omega) | \approx \left| (-1)^M (M!)^2 \frac{BN}{2} \frac{\sin \pi v}{\pi \prod_{n=-M}^{M} (v + n)} \right| \tag{99}$$

where

$$v = (\omega_0 - \omega)/\omega_a . \tag{100}$$

Suppose the largest† estimator is A_l and its largest immediate neighbor A_m. Of course $m - l = \pm 1$. Define

$$\alpha = m - l = \pm 1. \tag{101}$$

Let

$$a_1 = | A_l | \tag{102}$$

and

$$a_2 = | A_m | = | A_{l+\alpha} |. \tag{103}$$

Define

$$u = \frac{\omega_0}{\omega_a} - l; \quad -1/2 \leqq u \leqq 1/2. \tag{104}$$

Then from equation (99)

$$a_1 \approx (-1)^M (M!)^2 \frac{BN}{2} \frac{\sin \pi u}{\pi \prod_{n=-M}^{M} (u + n)} \tag{105}$$

† By largest we mean $| A_l | \geq | A_K |$ for $K \neq l$.

and

$$a_2 \approx (-1)^M (M!)^2 \frac{BN}{2} \frac{\sin \pi(u - \alpha)}{\pi \prod_{n=-M}^{M} (u + n - \alpha)} \tag{106}$$

since $\alpha = \pm 1$, equation (106) is the same as

$$a_2 \approx -(-1)^M (M!)^2 \frac{BN}{2} \frac{\sin \pi u}{\pi \prod_{n=-M-\alpha}^{M-\alpha} (u + n)} . \tag{107}$$

Division of equation (105) by equation (107) gives

$$\frac{a_1}{a_2} \approx -\frac{u - \alpha(M + 1)}{u + \alpha M} . \tag{108}$$

Define

$$u_1 = \frac{a_2(M + 1) - a_1 M}{a_1 + a_2} \tag{109}$$

then from equation (108) an estimate of u is

$$\hat{u} = \alpha u_1 . \tag{110}$$

Hence, the estimate of ω_0 is given by

$$\hat{\omega}_0 = \omega_a(l + \hat{u}). \tag{111}$$

From equation (105) the estimate of B is

$$\hat{B} = \frac{a_1 2\pi(-1)^M \prod_{n=-M}^{M} (\hat{u} - n)}{N(M!)^2 \sin \pi\hat{u}} , \tag{112}$$

where $\hat{u}$ is defined by equation (110).

Another version of equation (112), better for machine computation, is

$$\hat{B} = \frac{2a_1\pi\hat{u}}{N \sin (\pi\hat{u})} \prod_{n=1}^{M} 1 - \left(\frac{\hat{u}}{n}\right)^2 . \tag{113}$$

Method 2 with $M = 0$ is essentially the same as was derived by Penhune and Martin[14] to solve a radar problem.

5.3 *Method 3*

The simplicity of the estimation equations of Method 2 led us to extend this method to include any class of weighting functions described, in general form, by equations (37) and (38). We will refer to this more general method as Method 3.

From equations (109) and (110) we see that if a Class I weighting function is used, one way to obtain an estimate of u is to use the function

$$u_1 = \frac{Ca_2 - Da_1}{Ea_2 + a_1} \tag{114}$$

in equation (110). There are three degrees of freedom in the bilinear form and we chose to express them in the manner shown in equation (114).

Method 3 is simply the application of equation (114) to other classes of weighting functions. We obtained values for the coefficients in equation (114), for several weighting functions by:

(i) Computing a_1 and a_2, using equations (21), (63), (102), and (103), with $\Theta = 0$ and many values for ω_0 near $\omega_s/4$.

(ii) Computing the corresponding values of u from equation (104).

(iii) Choosing values for C, D, and E such that equation (114) gave a good fit to the data computed in the first two steps. It turns out that the curve described by equation (114) is satisfactory if it fits the computed data exactly at $u = 0$, $\frac{1}{4}$, and $\frac{1}{2}$.

In this manner we obtained the following coefficient values:

Class II weighting, $M = 7$, $R = 1000$;
$C = 1.96339$, $D = 1.01643$, $E = 0.893534$.

Class III weighting, $M = 2$; $C = 2.56919$,
$D = 1.5374$, $E = 1.06345$. For $M = 3$;
$C = 3.6020$, $D = 2.5862$, $E = 1.0317$.

Using an approximation similar to equation (71), but extended to include weighting functions described by equation (38), we obtain an estimate for B,

$$\hat{B} = \frac{2\pi a_1}{N \sin(\pi u_1)\left[\frac{1}{u_1} + \sum_{n=1}^{M} \frac{D_n u_1}{u_1^2 - n^2}\right]}. \tag{115}$$

Method 3 can be used with weighting functions specified only in terms of $H^*(\omega)$ as well as those given in terms of $H(\omega)$.

VI. COMPARISON OF ACCURACIES

In the preceding paragraphs we have derived several formulas that produce estimates of ω_0 and B from A_K values (estimators). We now turn to a comparison of these formulas on the basis of accuracy. The

accuracies we will compare do not include any possible computation or nonlinearity errors or other accuracy limitations that may be present in a DFT analysis system. Our accuracy comparisons include only the effects of leakage.

The estimators used in the simulations were generated by using the function $A(\omega)$, described by equation (63), in equation (21). This is equivalent to applying the weighting by multiplication in the time domain or by convolution in the frequency domain. The use of equation (63) in simulations greatly reduces computation time. All of the simulations used $N = 512$ and $f_s = N/T = 7040$ Hz.

All of the estimation methods presented above use approximations. In this section we shall demonstrate just how good the approximations are.

Consider the case where a tone of frequency f_0, angle θ_0, and amplitude B_0 is being measured while another tone, at frequency f_1, angle θ_1, and level B_1, is also being received. The presence of f_1 will affect the accuracy of any estimate one makes of f_0 or B_0 (due to leakage). The size of the errors in the estimates of f_0 and B_0 will depend upon which formula (method) is used and upon the values of f_0, B_0, θ_0, f_1, B_1, and θ_1. The combination of parameters that causes one method to give the worst estimates will, in general, not be the combination that causes another method to be at its worst. Thus it is difficult to compare methods.

We have compared the three methods on the basis of the worst estimates each will make when θ_0 and f_0 are confined to a specified range of values (for example, $990 \leqq f_0 \leqq 1003.75$ Hz and $0 \leqq \theta_0 \leqq 360$ degrees) and B_0, B_1, f_1, and θ_1 are fixed (for example, $B_0 = B_1 = 1$ and $\theta_1 = 0$ degrees).

Notice that if f_1 is equal to some multiple of $1/T$ then its A_K will be very small except for K near Tf_1. Thus such an f_1 cannot cause much error in any of the three methods of estimation of f_0, which use A_K values. For this reason we have fixed f_1 at a value that is an odd multiple of $\frac{1}{2}T$.

Tables V and VI illustrate how inaccurate frequency and level esti-

TABLE V—POOREST ESTIMATES WITH INTERFERENCE SEPARATION IN THE RANGE 55 ± 6.88 Hz, NO SPECIAL WEIGHTING

Method	Frequency Error, Hz	Magnitude Error, dB
1†	6.82	.596
2	7.37	.580

† Method 1 using only six estimators, those from $l - 2\alpha$ to $l + 3\alpha$.

TABLE VI—POOREST ESTIMATES WITH INTERFERENCE SEPARATION IN THE RANGE 178.96 ± 6.88 Hz, NO SPECIAL WEIGHTING

Method	Frequency Error, Hz	Magnitude Error, dB
1†	3.08	.0628
2	3.75	.165

† Method 1 using only six estimators.

mates are when no special weighting ($M = 0$) is used. The interfering tones corresponding to the simulations described in Tables V and VI were located at 1051.88 and 1175.63 Hz respectively. The frequency and magnitude error entries in these, and subsequent, tables give absolute values only.

The simulation results presented in Tables VII and VIII indicate that substantial improvement in the accuracy of frequency and magnitude estimates can be achieved when weighting is used. The data in Table VII shows that when the two tones are separated by a "small" frequency difference accurate frequency and level estimates can be obtained by using Method 3 with Class II or Class III weighting. Table VIII indicates that as the frequency separation increases Method 2 with Class I weighting is better. The accuracy of estimates made on closely spaced tones can, of course, always be improved by increasing N and T while keeping the ratio N/T constant.

It is interesting to note from Figs. 3 and 8 that, for a given value of

TABLE VII—POOREST ESTIMATES WITH INTERFERENCE SEPARATION IN THE RANGE 55 ± 6.88 Hz

Class I Weighting			
Method	M	Frequency Error, Hz	Magnitude Error, dB
1	1	.89	.11
1	2	3.32	.47
1	3	6.16	.96
2	1	.513	.12
2	2	.104	.11
2	3	.409	.5
Class II Weighting, R = 1000			
Method	M	Frequency Error, Hz	Magnitude Error, dB
1	7	1.14	.120
3	7	.0651	9.35E-3
Class III Weighting			
Method	M	Frequency Error, Hz	Magnitude Error, dB
1	2	2.11	.225
1	3	5.12	.821
3	2	.034	.026
3	3	.149	.0655

TABLE VIII—POOREST ESTIMATES WITH INTERERENCE SEPARATION IN THE RANGE 178.96 ± 6.88 Hz

Class I Weighting

Method	M	Frequency Error, Hz	Magnitude Error, dB
1	1	1.67E-3	2.79E-4
1	2	3.98E-4	5.25E-5
1	3	4.55E-2	4.70E-3
2	1	5.73E-3	1.42E-3
2	2	1.47E-4	2.19E-5
2	3	2.13E-5	1.55E-6

Class II Weighting, R = 1000

Method	M	Frequency Error, Hz	Magnitude Error, dB
1	7	5.56E-3	2.05E-5
3	7	8.09E-2	1.07E-2

Class III Weighting

Method	M	Frequency Error, Hz	Magnitude Error, dB
1	2	9.10E-5	1.19E-5
1	3	1.85E-2	1.90E-3
3	2	3.35E-3	3.24E-3
3	3	5.94E-4	9.62E-6

M, there is not a great deal of difference between the weighting contributed by $H_M(\omega)$ or $G_M(\omega)$. However, from Table VII it is obvious that the use of $G_2(\omega)$, when the tones are close together, will yield much more accurate estimates than Class I weighting.

In equation (101) the "pointer", α, was defined. The value of α is used by the system to determine whether the frequency being measured is above or below the frequency of the largest estimator, A_l. Our simulation studies showed that under certain circumstances α, as calculated by equation (101) will point in the wrong direction. In general this happens when the contributions to A_{l-1} and A_{l+1} due to the interference is equal to or greater than the difference in the contributions to the same estimators due to the tone being measured. Thus if $|A_{l-1}| \approx |A_{l+1}|$, a small difference in their magnitudes can change α. In our simulations this effect only caused trouble when f_0 and f_1 were separated by less than half the width of the main lobe of the weighting function, $H(\omega)$.

Since we have fixed $B_0 = B_1 = 1$ in the simulations we have ignored the adverse effects of "large" level differences on the accuracies of the various methods. Leakage from an interfering tone with a high level, relative to the tone of interest, would certainly tend to reduce the accuracy provided by any of the three methods, no matter which weighting is used.

VII. CONCLUSIONS

The discrete-tone measurement system we have been discussing is particularly well suited to systems that involve computer-controlled testing or measurement, provided the real time needed for the computations is available. Two advantages are:

(i) The only interface hardware is the A-D converter (with its lowpass filter).

(ii) The system is capable of measuring many received frequencies and levels during the same computation time.

For a given number of samples taken at a given sampling rate, the accuracy of the system can be significantly improved through the use of some type of weighting function. We have examined three classes of such smoothing functions and have developed formulas which permit the extraction of received signal frequencies and levels from the DFT coefficients. The results of system simulations, presented in Tables V through VIII, show that the inherent accuracy of the described system can, through the proper use of weighting functions and estimation methods, be made satisfactory for many applications.

With Method 2 considered to be a special case of Method 3, the tables show that the best estimation method, for all of the weighting functions examined, is Method 3.

The tables also show that there is no "best" weighting function. The weighting to be used for any particular application should be selected only after a consideration of the expected tone frequencies, the relative levels, the measurement accuracy desired, and the desired value for N. The sampling frequency, N/T, should be more than twice the highest frequency to be measured.

It is interesting to observe that the Taylor (Class II) weighting function used in the simulation is, *for the situations simulated*, not significantly better than the Class III weighting, $G_2(t)$, which is essentially that proposed by Blackman.[5] There may be other situations, however, when the nearly optimum main-lobe width of the Taylor functions is useful.

If the system could tolerate the relatively large amount of computer memory required, then the discrete Dolph–Chebychev functions described by equation (27) could provide some advantages.

VIII. ACKNOWLEDGMENTS

We are indebted to Messrs. D. R. Johnson, B. R. Saltzberg, and R. A. Smith for helpful discussions.

REFERENCES

1. Cochran, W. T., and others, "What is the Fast Fourier Transforms?," *IEEE Trans. Audio and Electroacoustics, AU-15,* No. 2 (June 1967), pp. 45–55.
2. Gentleman, W. M. and Sande, G., "Fast Fourier Transforms—for Fun and Profit," *American Federation of Information Processing Societies Proc., 29,* Washington, D. C.: Spartan, 1966, pp. 563–578.
3. Bergland, G. D., "A Guided Tour of the Fast Fourier Transform," *IEEE Spectrum, 6,* No. 7 (July 1969), pp. 41–52.
4. Papoulis, A., *The Fourier Integral and Its Applications,* New York: McGraw-Hill, 1962, pp. 48, 49.
5. Blackman, R. B. and Tukey, J. W., *The Measurement of Power Spectra,* New York: Dover, 1958, pp. 95–100.
6. Helms, H. D., "Nonrecursive Digital Filters: Design Methods for Achieving Specifications on Frequency Response," *IEEE Trans., AU–16,* No. 3 (September 1968), pp. 336–342.
7. Bingham, C., Godfrey, M. D., and Tukey, J. W., "Modern Techniques of Power Spectrum Estimation," *IEEE Trans. Audio and Electroacoustics, AU-15,* No. 2 (June 1967), pp. 56–66.
8. Dolph, C. L., "A Current Distribution for Broadside Arrays which Optimizes the Relationship between Beam Width and Side-Lobe Level," *Proc. IRE, 34,* No. 6 (June 1946), pp. 335–348.
9. Cook, C. E. and Bernfeld, M., *Radar Signals—An Introduction to Theory and Application,* New York: Academic Press, 1967, pp. 178–182.
10. Taylor, T. T., "Design of Line-Source Antennas for Narrow Beamwidth and Low Side Lobes," *IRE Trans., AP-3,* No. 1 (January 1955), pp. 16–28.
11. Klander, J. R., and others, "Theory and Design of Chirp Radars," B.S.T.J., *39,* No. 4 (July 1960), pp. 782–790.
12. Kuo, F. F. and Kaiser, J. F., *Systems Analysis by Digital Computer,* New York: Wiley, 1966, Chapter 7.
13. Larsen, A. G. and Singleton, R. C., "Real-Time Spectral Analysis on a Small General-Purpose Computer," *1967 Fall Joint Computer Conf., AFIPS Proc.,* Washington, D. C.: Spartan, 1967, pp. 665–674.
14. Penhune, J. P. and Martin, L. R., "Determination of Doppler Velocity and Ballistic Coefficient from Coherent Radar Data," ESD-TDR-65-41, Technical Rept. 378, M.I.T. Lincoln Labs., Lexington, Mass., pp. 11–53.